Biochemistry

 Volume 35, Number 42 October 22, 1996

Articles

Identification of Adenine Binding Domain Peptides of the $NADP^+$ Active Site within Porcine Heart $NADP^+$-Dependent Isocitrate Dehydrogenase†

Banumathi Sankaran,‡ Ashok J. Chavan,§ and Boyd E. Haley*

Division of Medicinal Chemistry and Pharmaceutics, College of Pharmacy, University of Kentucky Medical Center, Lexington, Kentucky 40536-0082

Received June 19, 1996; Revised Manuscript Received August 6, 1996⊗

ABSTRACT: Photoaffinity labeling with [2′-^{32}P]2$N_3$$NADP^+$ and [^{32}P]2$N_3$$NAD^+$ was used to identify two overlapping tryptic and chymotryptic generated peptides within the adenine binding domain of $NADP^+$-dependent isocitrate dehydrogenase (IDH). Photolysis was required for insertion of radiolabel, and prior photolysis of photoprobes before addition of IDH prevented insertion. Photoincorporation of 2$N_3$$NAD^+$ inhibited the enzymatic activity of IDH. Photolabeling of IDH with both [^{32}P]2$N_3$$NAD^+$ and [2′-^{32}P]2N_3-$NADP^+$ showed saturation effects with apparent K_ds of 20 and 14 μM (±12%), respectively. The efficiency of photoincorporation at saturation of binding sites was determined to be about 50%. Also, photolabeling was observed with [^{32}P]8N_3ATP and [^{32}P]2N_3ATP but with saturation effects observed at lower affinity. With all radiolabeled probes reduction of photoinsertion was effected best by the addition of $NADP^+$ followed by NAD^+ and then ATP, indicating that photoinsertion with all the probes was within the $NADP^+$ binding site. Isolation of [^{32}P]2$N_3$$NAD^+$ and [2′-^{32}P]2$N_3$$NADP^+$ photolabeled peptides by use of immobilized boronate and immobilized Al^{3+} chromatography, respectively, followed by HPLC purification resulted in the identification of overlapping peptides corresponding to Ile^{244}-Arg^{249} and Leu^{121}-Arg^{133} (tryptic fragments) and Lys^{243}-His^{248} and Leu^{121}-His^{135} (chymotryptic fragments). Trp^{125} and Trp^{245} were identified as the sites of photoinsertion based on these residues not being detectable on sequencing, the lack of chymotryptic cleavage at these residues, and the decreased rate of trypsin digestion at nearby Lys^{243} and Lys^{127}. Sequence analysis of [^{32}P]8N_3ATP and [^{32}P]2N_3ATP photolabeled peptides gave essentially the same peptide regions being photolabeled but at much lower efficiency, indicating that the effects of ATP on IDH activity are dependent on competition for the same site.

Our laboratory has been identifying the peptides of the purine ring binding domain of several ATP, GTP, and NAD^+/$NADP^+$ binding proteins. This report concerns $NADP^+$-dependent isocitrate dehydrogenase (IDH), an enzyme of the citric acid cycle which is present in all mammalian species. IDH catalyzes the oxidative decarboxylation of isocitrate to α-ketoglutarate and is a key step in aerobic metabolism. Mammalian heart tissues contain two forms of IDH, a NAD^+-dependent IDH [isocitrate:NAD^+ oxidoreductase (decarboxylating), EC 1.1.1.41] and the $NADP^+$-dependent IDH (EC 1.1.1.42). Both these enzymes are found in the mitochondria with the $NADP^+$-dependent enzyme also being found in the cytosol of many tissues. Mitochondrial NAD^+-dependent IDH is considered a primary regulatory enzyme and proposed to be allosterically regulated

† This work was supported by National Institutes of Health Grant GM-35766 and the Lexington Clinic Foundation.

* Corresponding author: Boyd E. Haley, Medicinal Chemistry, College of Pharmacy, University of Kentucky Medical Center, Lexington, KY 40536-0082. FAX: (606) 257-2489; E-mail: BEHALEY@POP.UKY.EDU.

‡ Present address: Department of Biochemistry, University of Rochester Medical Center.

§ Present address: Research Products, Int., 410 N. Business Center Dr., Mt. Prospect, IL 60056.

⊗ Abstract published in *Advance ACS Abstracts,* October 1, 1996.

S0006-2960(96)01459-6 CCC: $12.00

by energy charge through activation by ADP, and inhibition by ATP, NADH, and NADPH. However, $NADP^+$-IDH is a dimer of identical subunits (Kelly & Plaut, 1981) and is not known to be allosterically regulated (Kornberg & Pricer, 1951), and uses a metal−isocitrate complex as the substrate (Colman, 1983). The kinetics have been thoroughly studied and shown to proceed through a random sequential process with catalysis more rapid than product release (Uhr et al., 1974; Northrop & Cleland, 1974). The complete metabolic functions of $NADP^+$-dependent IDH and several structural features remain unclear. However, the enzyme has been extensively studied and was recently reviewed (Colman, 1989).

Mammalian $NADP^+$-IDH may be contrasted to the *Escherichia coli* form of $NADP^+$-IDH which is regulated by phosphorylation at Ser^{113}. This phosphorylation inhibits the enzyme and controls the rates between the glyoxalate bypass and the citric acid cycle (LaPorte & Koshland, 1983). Also, the structure of *E. coli* $NADP^+$-IDH has been solved and refined at 2.5 Å (Hurley et al., 1989). Also, structures of *E. coli* $NADP^+$-IDH−Mg^{2+}−isocitrate complex (Hurley et al., 1991), IDH−Ca^{2+}−isocitrate−$NADP^+$ complex (Stoddard & Koshland, 1993a), and IDH−Ca^{2+}−α-ketoglutarate−NADPH (Stoddard & Koshland, 1993b) have all been solved at 2.7 Å resolution. However, to date neither of the crystal structures of mammalian NAD^+- or $NADP^+$-dependent IDH has been reported. Knowledge about NAD^+/$NADP^+$ binding site peptides should be considered important structural information that is needed to broaden our understanding of the mechanisms of catalytic activity of dehydrogenases. Additionally, identification of binding site peptides enables structural comparisons between species such as eukaryotic versus prokaryotic $NADP^+$-dependent IDHs or between various forms of eukaryotic $NADP^+$-dependent IDH and respective NAD^+-dependent IDHs.

$NADP^+$-IDH from pig heart mitochondria is a dimer of identical 46 600 Da subunits whose 413 amino acid sequence has been determined by isolation and translation of a cDNA encoding region which showed 63% amino acid sequence homology with yeast mitochondrial $NADP^+$-IDH and only 14% sequence homology with *E. coli* $NADP^+$-IDH (Haselbeck et al., 1992). A divalent metal ion is required for $NADP^+$-IDH activity, the highest being obtained with Mn^{2+} (Coleman, 1972; Bailey & Colman, 1987). The metal−isocitrate complex is thought to be the actual substrate for this enzyme (Colman, 1983), and a peptide region of the metal isocitrate binding site of porcine $NADP^+$-dependent IDH has been identified by affinity cleavage of the enzyme by Fe^{2+}−isocitrate complex (Soundar & Colman, 1993). Asp^{253} and His^{309} were suggested to be the coordination sites for Fe^{2+}−isocitrate, and Tyr^{272}-Asp^{273} were suggested as residues involved in the coordination site for the free metal.

Identification of nucleotide binding domains of enzymes is important for structural studies that may add to our understanding of the mechanism of action. Recently, a glutamyl peptide, Asp^{376}-Leu^{387}, was identified using the substrate analog 3-bromo-2-ketoglutarate (Erlich & Colman, 1987). The same peptide was also isolated using a chemically reactive affinity label for $NADP^+$, 2-[(bromo-2,3-dioxobutyl)thio]-1,N^6-ethenoadenosine (Bailey & Colman, 1987). This reagent incorporated into 0.5 mol/mol of enzyme or one subunit per dimer, and the modification was proposed to be within the coenzyme site.

A corresponding approach has been to use photoaffinity reagents to identify the base binding domains of nucleotide binding proteins. For example, [^{32}P]$2N_3NAD^+$ (see footnote 1) has been used to identify the adenine ring domain peptides of the NAD^+ binding site of glutamate dehydrogenase and lactate dehydrogenase (Kim & Haley, 1990, 1991), prolactin (Trad et al., 1993), and *C. botulinum* C3 ADP-ribosyltransferase (Chavan et al., 1992). Recently, [2′-^{32}P]$2N_3NADP^+$ was used to photolabel microsomal steroid 5α-reductase and identify the subunit involved in $NADP^+$ binding and to monitor the purification of the enzyme 5α-reductase throughout the purification procedure as well as identify a peptide of the adenine binding domain of the NADP(H) binding site (Bhattacharyya et al., 1994, 1995). Immobilized Al^{3+} chelate affinity chromatography, which has specific high affinity for phosphate containing peptides, has recently been used to isolate and identify the [^{32}P]$8N_3$GTP photolabeled peptides of the GTP site of β-tubulin (Jayaram & Haley, 1994) and glutamate dehydrogenase (Shoemaker & Haley, 1993), the [α-^{32}P]$8N_3$ADP photolabeled peptides of the ADP activating site of glutamate dehydrogenase (Shoemaker & Haley, 1996), and the [^{32}P]$2N_3$ATP and [^{32}P]$8N_3$ATP photolabeled peptides of the ATP site of creatine kinase (Olcott et al., 1994). Recent crystallography studies confirmed that the two peptides identified in creatine kinase (Olcott et al. 1994) are in the adenine binding domain (Fritz-Wolf et al., 1996). In the present study, [2′-^{32}P]$2N_3NADP^+$, [^{32}P]$2N_3NAD^+$, [^{32}P]$8N_3$ATP, and [^{32}P]$2N_3$ATP were used to study $NADP^+$-dependent IDH and identify the peptide sequences in the adenine binding domain of the $NADP^+$ site.

MATERIALS AND METHODS

The synthesis and purification of [^{32}P]$2N_3NAD^+$, [2′-^{32}P]$2N_3NADP^+$, and α- and γ-^{32}P-labeled $2N_3$ATP and $8N_3$-ATP probes were done as previously reported (Kim & Haley, 1990; Salvucci et al., 1992; Potter & Haley, 1982) or they were obtained from Research Products Int., Mt. Prospect, IL. The NAD^+ and $NADP^+$ probes were prepared at a specific activity of 1−4 mCi/μmol, and the ATP probes varied between 9 and 20 mCi/μmol. Porcine heart $NADP^+$-dependent IDH was from two sources, Sigma and Boehringer Mannheim. Molecular weight standards were obtained from Bio-Rad. Trypsin, chymotrypsin, and all other reagents were from Sigma Chemical Co. or Promega and were sequencing grade.

Photolabeling of IDH. For saturation studies, samples containing 1−2 μg of IDH in 10 mM MES, pH 6.0, in a total volume of 50 μL were incubated with increasing concentrations of [2′-^{32}P]$2N_3NADP^+$ or other ^{32}P-labeled photoprobes for 30 s. The specific activity of the probes was reduced 10-fold in saturation versus protection experiments to decrease the amount of radiolabeled compound used. The samples were irradiated with a hand-held 254 nm Mineralight UVS-11 UV lamp (I = 3400 μW/cm^2) for 60 s from a distance of 4 cm at 4 °C. After photolysis, the reaction was quenched by addition of 35 μL of protein solubilizing mixture containing 10% SDS, 3.6 M urea, 162

[1] Abbreviations: $8N_3$ATP, 8-azidoadenosine 5′-triphosphate; $8N_3$-ADP, 8-azidoadenosine 5′-diphosphate; $2N_3$ATP, 2-azidoadenosine 5′-triphosphate; $2N_3NAD^+$, nicotinamide 2-azidoadenine dinucleotide; $2N_3NADP^+$, nicotinamide 2-azidoadenine dinucleotide phosphate; PTH, phenylthiohydantoin; SDS, sodium dodecyl sulfate.

mM dithiothreitol, pyronin-Y, and 20 mM Tris, pH 8.0. The samples were then subjected to SDS−PAGE. Apparent K_ds for each photoprobe are from the average of three or more experiments and were determined by the concentration of probe that gave one-half maximum photoinsertion in the absence of competing nucleotide.

For protection studies, 1−2 μg of IDH in 10 mM MES, pH 6.0, was incubated for 60 s with increasing concentrations of the competitor nucleotide in a total volume of 50 μL. After the incubation, 10 μM [2′-^{32}P]2N_3NADP$^+$, or other photoprobe (of highest available specific activity), was added to the reaction mixture and incubated for 30 s, and then photolyzed for 60 s. After photolysis, the reaction was quenched by the addition of 35 μL of the protein solubilizing mixture, the proteins were separated by SDS−PAGE, and the amount of radiolabel was determined. The apparent K_ds of the protecting compounds were determined by the concentration of compound needed to reduce photoinsertion by 50% of the maximum. All apparent K_ds reported are the average of no less than three different experiments, and standard errors were determined using Sigma Plot.

Determination of IDH Activity. Enzyme assays were done at 25 °C in 1 mL volumes containing 20 mM Tris-HCl buffer (pH 7.4), 0.1 mM $NADP^+$, 4 mM isocitrate, and 2 mM $MnSO_4$. Monitoring was done at 340 nm to measure the reduction of $NADP^+$, which was determined to be linear for over 6 min.

SDS−Polyacrylamide Gel Electrophoresis. After solubilization, the photolabeled samples were subjected to electrophoresis on a 10% separating gel with 4% stacking gel, which is slightly modified from previously reported procedures (Laemmli, 1970; Haley, 1975). The gel was stained with Coomassie Brilliant Blue R and destained for 12 h. The gel was then dried on a slab gel drier, and the dried gel was subjected to autoradiography. ^{32}P incorporation was quantified by excision of bands from the gel followed by scintillation counting in a Packard Minaxi Tri-Carb liquid scintillation system, Model B4430 (counting efficiency, 99% for ^{32}P). Alternatively, the gel was scanned in a Ambis 4000 radioisotope detector to determine the ^{32}P incorporation into the protein bands.

Photolabeling and Enzymatic Digestion of IDH. Determination of the site modified by each of the respective analogs was done by incubating 0.1−1.0 mg of IDH, as indicated, in 10 mM MES, pH 6.0, and the designated amounts of the photoprobe being used. For example, with [2′-^{32}P]2N_3NADP$^+$, 500 μg of IDH in 10 mM MES, pH 6.0, was incubated with 35 μM [2′-^{32}P]2N_3NADP$^+$ (total volume of 750 μL) for 30 s at 4 °C. The mixture was irradiated for 90 s. After photolysis, 35 μM [2′-^{32}P]2N_3NADP$^+$ was added again and incubated for 30 s, followed by photolysis for 90 s. After the second photolysis, the reaction was quenched by the addition of an equal volume of cold 7% perchloric acid (final concentration of 3.5%). The mixture was transferred to a 15 mL Corex test tube and kept at 4 °C for 30 min. The protein was precipitated by centrifugation at 2000 rpm for 20 min in a Beckman Model TJ-6 centrifuge at 0 °C. The supernatant was drawn off, and the pellet was resuspended in 10 mM ammonium bicarbonate containing 2 M urea. The pH was adjusted to 8.0 by the addition 1 M NH_4OH.

IDH was proteolyzed by the addition of 20 μg of trypsin or chymotrypsin and kept at 25 °C for 3 h, after which 20 μg of the respective protease was added again, and the digestion mix was kept at 25 °C overnight.

Immobilized Metal Affinity Chromatography. The resin (0.5−1 mL), iminodiacetic acid−epoxy activated Sepharose 6B fast flow (Sigma), was prepared for affinity chromatography by washing successively with water, 20 mL of 50 mM $AlCl_3$, 15 mL of water, and 20 mL of 50 mM ammonium acetate, pH 6.0 (buffer A). The digested protein was diluted with 8−10-fold with buffer A, the pH adjusted to 6.0, loaded on to the column, and washed with 20 mL of buffer A. The photolabeled peptides were eluted with 5−10 mL of 10−15 mM K_2HPO_4 in 50 mM ammonium acetate, pH 8.0. During chromatography, 1.5 mL fractions were collected and the radioactivity was determined by liquid scintillation counting.

Immobilized Boronate Chromatography. This was done as previously described (Chavan et al., 1992). Affi-Gel 601 (Bio-Rad Laboratories) resin was equilibrated with 100 mM ammonium acetate, pH 8.9 (buffer B). The digested protein was diluted 8−10-fold with buffer B and loaded onto a column containing 2 mL of the resin. The column was washed successively with 10 mL of buffer B, 10 mL of buffer B containing 0.5 M NaCl, 10 mL of buffer B, 10 mL of buffer B containing 4 M urea, and 10 mL of buffer B. The photolabeled peptides were eluted with 50 mM ammonium acetate containing 100 mM sorbitol, pH 8.9, with 1.5 mL fractions being collected. Radioactivity was determined by liquid scintillation counting.

Reversed Phase HPLC. The photolabeled peptides purified from the immobilized metal or immobilized boronate affinity chromatography were further purified by low flow rate (0.5 mL/min) reversed phase HPLC on an Aquapore RP 300 C8 column (Brownlee Laboratory) on an LKB HPLC system. The gradient used was 0% solvent B at 10 min and 100% solvent B at 70 min (solvent A: 0.1% trifluoroacetic acid; solvent B: 70% acetonitrile, 0.09% trifluoroacetic acid). The UV absorbance of the eluted peptides was monitored by a diode array spectral detector, and the radioactivity in the collected 0.5 mL fractions was determined by Cerenkov liquid scintillation counting. The fractions containing radioactivity and indicating corresponding absorbance at 214 nm were analyzed on an Applied Biosystems 477A protein sequencer with an on-line PTH identification, at the University of Kentucky Macromolecular Structure Facility.

Confirmation of site-specific photolabeling and identification of peptide regions using the immobilized Al^{3+} or boronate columns and the HPLC procedure above was done by photolyzing IDH with radiolabeled photoprobe in the presence of protective nucleotide and showing reduced isolation of photolabeled peptide.

RESULTS

All studies were done using porcine heart mitochondrial $NADP^+$-IDH. All experiments using [α-^{32}P]8N_3ATP, [γ-^{32}P]2N_3ATP, [2′-^{32}P]2N_3NADP$^+$, and [α-^{32}P]2N_3NAD$^+$ to demonstrate photolysis requirement and lack of pseudophotoaffinity labeling, and to determine optimal photoinsertion conditions, saturation effects, and reduction of photoinsertion, were repeated at least three times. Initial studies were conducted over a pH range of 5.0−8.5 using Tris and MES buffering systems. The effects of changing pH were minimal between values of 5.5 and 7.0 with MES buffer, pH 6.0, giving maximum photoinsertion of [^{32}P]8N_3ATP, [^{32}P]2N_3-

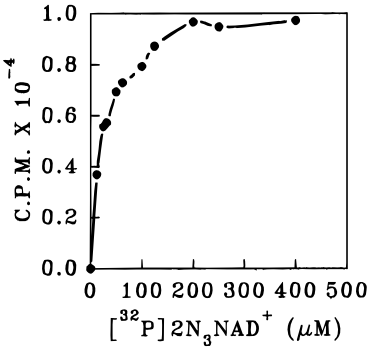

FIGURE 1: Saturation of photinsertion of [^{32}P]2N$_3$NAD$^+$ into IDH. One microgram of IDH in a total volume of 50 μL was photolyzed as given in Materials and Methods with increasing concentrations of [^{32}P]2N$_3$NAD$^+$ (SA = 0.198 mCi/μmol) as indicated. Protein was separated by SDS−PAGE, the gel stained and dried, and ^{32}P-radiolabel detected and quantified by an Ambiss 4000 β-detector.

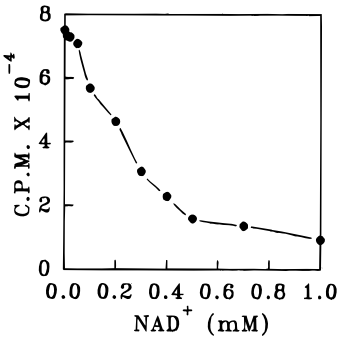

FIGURE 2: Reduction of [^{32}P]2N$_3$NAD$^+$ photoinsertion into IDH by increasing concentrations of NAD$^+$. One microgram of IDH in 50 μL total volume was incubated as given in Materials and Methods with 10 μM [^{32}P]2N$_3$NAD$^+$ (SA = 3.96 mCi/μmol) in the presence of the indicated concentrations of NAD$^+$ and photolyzed. Level of incorporation of ^{32}P-radiolabel was determined as given in Figure 1.

NAD$^+$, and [2′-^{32}P]2N$_3$NADP$^+$ into IDH. However, a rapid decline in photoinsertion occurred after pH 7.5 with less than 12% remaining at pH 8.5. Also, as expected, photoinsertion was increased at lower ionic strengths. Consistently, regardless of the photoprobe used, NADP$^+$ gave the most effective reduction of photoinsertion followed by NAD$^+$ then ATP.

The specificity of [^{32}P]8N$_3$ATP, [^{32}P]2N$_3$NAD$^+$, and [2′-^{32}P]2N$_3$NADP$^+$ interactions was demonstrated by the following. Photoinsertion of the azidonucleotide exhibited activating UV light dependency and showed saturation effects. Increasing ATP, NAD$^+$, or NADP$^+$ concentrations decreased photoinsertion of [^{32}P]2N$_3$NAD$^+$ or [2′-^{32}P]-NADP$^+$ in close agreement with the known affinity of ATP, NAD$^+$, or NADP$^+$ for IDH. When the sample was not irradiated, no incorporation of ^{32}P was observed (data not shown). This demonstrated the absence of enzymatic incorporation of radiolabel from [^{32}P]8N$_3$ATP and [2′-^{32}P]2N$_3$NADP$^+$ under these conditions. When the photoprobes were preirradiated followed by immediate addition of IDH, no covalent modification was observed (data not shown). This demonstrates an absence of any light generated, long-lived chemical intermediates such as the dehydroazephines generated by photolysis of phenyl azides. These intermediates would cause pseudophotoaffinity labeling, which would increase the possibility of modification outside of the NADP$^+$ binding site as is observed using classical, long half-life chemical probes.

Saturation of [^{32}P]8N$_3$ATP, [^{32}P]2N$_3$ATP, [^{32}P]2N$_3$NAD$^+$, and [2′-^{32}P]2N$_3$NADP$^+$ photoinsertion into IDH occurred with apparent K_ds of 33 ± 4, 25 ± 3, 20 ± 3, and 14 ± 3 μM, respectively. Figure 1 shows the saturation of [^{32}P]2N$_3$-NAD$^+$ photoinsertion and is representative of data obtained using each of the photoprobes. The efficiency of photoincorporation of [2′-^{32}P]2N$_3$NADP$^+$ into IDH at saturation (185 μM) was approximately 50% as determined by excising a known quantity of photolabeled IDH from a SDS−PAGE and determining the amount of probe photoinserted by liquid scintillation counting. Photoinsertion of [^{32}P]2N$_3$NAD$^+$ and [^{32}P]8N$_3$ATP showed saturation effects near 200 μM (data not shown). Apparent in these experiments were the increased affinities of the azidopurine analogs compared to their native counterparts. However, this has been observed several times with other NAD$^+$ or NADP$^+$ binding proteins (Kim & Haley, 1990, 1991; Bhattacharyya et al., 1994, 1995; Chavan et al., 1992; Trad et al., 1993). The contribution of the azidopurine moiety to the free energy of binding appears to dominate other contributions from the ribose and phosphate groups, enhancing the affinity of each azido probe.

Table 1: Effects of Photolysis and Photolabeling with [^{32}P]2N$_3$NAD$^+$ on the Enzyme Activity of IDH

photolysis[a]	[^{32}P]2N$_3$NAD$^+$ [b]	NAD$^+$ [c]	ΔOD$_{340}$[d]	% control[e]
−	−	−	0.91	100
+	−	−	0.91	100
−	+	−	0.89	97
−	+	+	0.80	88
+	+	−	0.46	51
+	+	+	0.84	93

[a] Photolysis was for 60 s at 0 °C. [b] 130 μM concentration. [c] 800 μM concentration. [d] Determined after 4 min incubation. [e] Sample not treated used as control.

A representative protection study is shown in Figure 2 and demonstrates that about 600 μM NAD$^+$ was able to reduce photoinsertion of 10 μM [^{32}P]2N$_3$NAD$^+$ by 80% with an apparent K_d of 200 ± 25 μM. The K_d of NAD$^+$ binding obtained from protection experiments was higher than the K_d for [^{32}P]2N$_3$NAD$^+$ (20 ± 3 μM) obtained from saturation studies. This is probably due to the tighter binding affinity for 2N$_3$NAD$^+$ compared to that for NAD$^+$. The higher affinity of 2N$_3$NAD$^+$ versus NAD$^+$ was confirmed by experiments showing that 100 μM 2N$_3$NAD$^+$ reduced [2′-^{32}P]2N$_3$NADP$^+$ photoinsertion more effectively than 100 μM NAD$^+$ (data not shown). This phenomenon was also observed for glutamate and lactate dehydrogenase (Kim & Haley, 1990). In other protection experiments, both [2′-^{32}P]2N$_3$NADP$^+$ and [^{32}P]8N$_3$ATP photoinsertion could be reduced over 90% by low μM levels of NADP$^+$, NAD$^+$, and ATP. However, NADP$^+$ always reduced these photoinsertions most effectively, as expected for competitive binding at the NADP$^+$ site (data not shown). The results of several similar experiments consistently demonstrated that photolabeling by [2′-^{32}P]2N$_3$NADP$^+$ was specific for the NADP$^+$ binding site of IDH and indicated that [^{32}P]2N$_3$-NAD$^+$, [^{32}P]8N$_3$ATP, and [^{32}P]2N$_3$ATP were also binding at the NADP$^+$ site but with less affinity.

The effect of photoinsertion of 2N$_3$NAD$^+$ on the ability of IDH to convert NADP$^+$ to NADPH is shown in Table 1. Photolysis alone under these conditions did not detectably affect IDH activity. Addition of 2N$_3$NAD$^+$ without photolysis reduced activity about 3% whereas with photolysis a

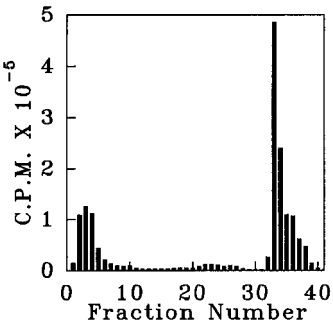

FIGURE 3: Isolation of [2′-^{32}P]2N$_3$NADP$^+$ photolabeled peptides by immobilized Al^{3+} affinity chromatography. 500 μg of IDH was photolableled twice with 30 μM [2′-^{32}P]2N$_3$NADP$^+$, proteolyzed with trypsin and loaded onto an immobilized Al^{3+} affinity column as described in Materials and Methods. Fractions 1−4 represent flow-through factions which contain non-photolabeled peptides, fractions 5−15 represent wash fractions, and fractions 16−19 represent phosphate eluted peptides.

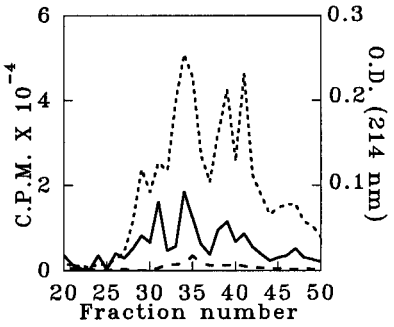

FIGURE 4: HPLC separation of tryptic peptides produced from [^{32}P]2N$_3$NAD$^+$ photolabeled IDH after isolation from an immobilized boronate affinity column by sorbitol. IDH (1 mg) was photolabeled twice with 50 μM [^{32}P]2N$_3$NAD$^+$ in the presence or absence of 1 mM NAD$^+$ and proteolyzed by trypsin, and the photolabeled peptides were isolated from bulk peptides by immobilized boronate chromatography. Sorbitol eluted peptides were separated by reversed phase HPLC as given in Materials and Methods. The bottom dashed and top dashed lines are the ^{32}P levels obtained with and without NAD$^+$ present during photolysis, respectively. The solid line is the OD$_{214}$ absorbance profile of peptides produced without NAD$^+$ present. No detectable OD$_{214}$ peaks were obtained when NAD$^+$ was present.

49% loss of enzyme activity occurred. The presence of 800 μM NAD$^+$ reduced this photodependent inhibition, giving 93% of the original activity. In addition, analysis of [^{32}P] incorporation into IDH after SDS−PAGE indicated that about 50% of the IDH subunits were photolabeled. This indicates that IDH represents a dehydrogenase that is most effectively photolabeled, forming a chemically stable photoinsertion product. This is probably due to the insertion being into an aromatic amino acid as indicated by the sequencing data. In the absence of activating light, increasing concentrations of NAD$^+$ and 2N$_3$NAD$^+$ inhibited the activity of IDH (data not shown) in agreement with earlier reported results (Erlich & Colman, 1978).

To identify the peptide sequences that were photomodified by [^{32}P]2N$_3$NAD$^+$, [2′-^{32}P]2N$_3$NADP$^+$, [^{32}P]8N$_3$ATP, and [^{32}P]2N$_3$ATP, IDH was first photolabeled twice with each probe, respectively. Concentrations of probes used were always below the saturation values to reduce any nonspecific photolabeling. Photolabeled IDH was separated from most of the noncovalently bound nucleotide by PCA precipitation. The photomodified IDH was dissolved in ammonium bicarbonate−urea, pH 8.0 (see Materials and Methods), and digested with trypsin overnight. Since the presence of the 2′-phosphate blocked the *cis*-hydroxyls from interacting with boronate, the [2′-^{32}P]2N$_3$NADP$^+$ and [^{32}P]8N$_3$ATP photolabeled IDH peptides were separated from nonphotolabeled peptides using immobilized Al^{3+} affinity chromatography. [^{32}P]2N$_3$NAD$^+$ photolabeled peptides (which do not bind effectively to immobilized Al^{3+} columns) were separated from nonphotolabeled peptides using immobolized boronate chromatography. With immobilized Al^{3+} chromatography over 90% of the added radioactivity was recovered in the P$_i$ eluted fractions. With boronate chromatography about 80% of the radioactivity was eluted with sorbitol.

Figure 3 shows a typical radioactivity profile of the flow-through, washes, and P$_i$ elution fractions from the immobilized Al^{3+} affinity chromatographic procedure. In this experiment, two photolyses with 30 μM [2′-^{32}P]2N$_3$NADP$^+$ were used to modify 500 μg of IDH. A very small percentage of the radioactivity was observed eluting in the flow-through and washes (fractions 1−15) whereas greater than 90% of the total radioactivity coeluted with the first four P$_i$ eluate fractions (fractions 16−19). The flow-through (fractions 1−5) and the P$_i$ eluate (fractions 16−19) were pooled separately and concentrated in preparation for reversed phase HPLC.

When the flow-through fractions from either the immobilized Al^{3+} or boronate columns were subjected to reversed phase HPLC, a complex UV absorbing profile containing many peptides was obtained as expected (data not shown). However, no radioactive peaks were observed in the profile of the flow-through fractions. The peptide peaks observed in this profile represent the nonphotolabeled peptides which do not bind to either the immobilized Al^{3+} or boronate affinity columns. This profile is very similar to that obtained when the entire tryptic digest of IDH is subjected to HPLC (data not shown).

The results of Figure 4 show that addition of 1 mM NAD$^+$ during photolysis greatly reduces the amount of photolabeled tryptic peptides isolated by HPLC when 50 μM [^{32}P]2N$_3$-NAD$^+$ was the photoprobe and immobilized boronate chromatography was used to first separate the photolabeled peptides (the only ones with *cis*-hydroxyls) from the nonphotolabeled peptides. The boronate column was washed with 0.5 M NaCl and 4 M urea to remove all nonphotolabeled peptides. The photolabeled peptides, covalently attached through the immobolized boronate−*cis*-hydroxyl bonds, were eluted using sorbitol as a competing diol at pH 8.9. HPLC profiles of the radioactivity and absorbance (214 nm) showed four major radioactive peaks with maxima at fractions 10, 34, 39, and 41. Fraction 10, which represents the apex of the flow-through and elutes before starting the acetonitrile gradient, did not contain any peptide, and the radioactivity eluting in this position has been previously demonstrated to be primarily due to unbound nucleotide not removed by the PCA precipitation step (Jayaram & Haley, 1994; Shoemaker & Haley, 1993). However, radioactivity eluting with fractions 34, 39, and 41 was reduced by over 95% by the presence of NAD$^+$. For each of these three peaks only the single tube at the apex of each radioactive peak (i.e., fractions 34, 39, and 41) was collected and concentrated under reduced pressure for sequence analysis. Radioactivity levels in each tube allowed for the prediction of the number of picomoles of peptide present using the assumption of one peptide per

Table 2: Sequence Analysis of the Photolabeled Tryptic Peptides of IDH Photolabeled with [^{32}P]2N$_3$NAD$^+$ and [2′-^{32}P]2N$_3$NADP$^+$ after HPLC Purification

	[^{32}P]2N$_3$NAD$^+$						[2′-^{32}P]2N$_3$NADP$^+$					
	fr[a] 34		fr 39		fr 41		fr 33		fr 36		fr 39	
cycle												
1	I^{244} [b]	(761)[c]	L^{121}	(26)	L^{121}	(577)	I^{244}	(86)	Y^{242}	(32)	L^{121}	(24)
2	W^{245}	(0)	V	(54)	V	(452)	W	(0)	K	(19)	V	(25)
3	Y	(784)	P	(118)	P	(714)	Y	(59)	I	(25)	P	(24)
4	E	(432)	G	(51)	G	(298)	E	(52)	W^{245}	(0)	G	(22)
5	H	(125)	W^{125}	(0)	W^{125}	(11)	H	(5)	Y	(15)	W^{125}	(1)
6	R^{249}	(226)	T	(13)	T	(113)	R^{249}	(11)	E	(19)	T	(7)
7			K^{127}	(6)	K^{127}	(194)			H	(2)	K^{127}	(7)
8					P	(144)			R^{249}	(7)	P	(5)
9					I	(146)					I	(6)
10					T	(61)					T	(5)
11					I	(122)					I	(6)
12					G	(78)					G	(7)
13					R^{133}	(42)					R^{133}	(5)

[a] fr, fraction no. [b] Superscript numbers identify primary sequence location. [c] Numbers in parentheses are picomoles of residue obtained.

molecule of radiolabeled probe and an efficiency of 27.2% by Cherenkov ^{32}P counting.

The amino acid sequence obtained from each of these fractions is summarized in Table 2. Fraction 34 contained about 750 pmol of the peptide Ile^{244}-Arg^{249}, with Trp^{245} not being detectable. Fraction 39 contained about 50−100 pmol of the peptide corresponding to Leu^{121}-Lys^{127} with Trp125 not being detected. An extended species of Leu^{121}-Lys^{127} was found in fraction 41 which contained in excess of 450 pmol of the peptide Leu^{121}-Arg^{133}. Recovery of Trp^{125} was greatly decreased (298 to 11 pmol), and Lys^{127} in this peptide was not cleaved by trypsin.

An identical HPLC analysis was done of photolabled tryptic peptides eluted from an immobilized Al^{3+} column where 30 μM [2′-^{32}P]2N$_3$NADP$^+$ was used to modify IDH. In this experiment, equal amounts of IDH were photolabeled with and without competing 1 mM NADP$^+$ being present. The results showed that NADP$^+$ almost totally prevented photolabeling of IDH peptides (data not shown). Further, the number and retention times of the [2′-^{32}P]2N$_3$NADP$^+$ photolabeled peptides were similar to those observed using [^{32}P]2N$_3$NAD$^+$ and immobilized boronate chromatography. However, the efficiency of photoinsertion appeared much better using [^{32}P]2N$_3$NAD$^+$ as determined by the UV absorbance levels and the subsequent sequencing results. Again, the first peak was eluted at fraction 10 before the start of the acetonitrile gradient and contained no detectable peptides as expected. Fraction 33 was the apex of the second peak and contained about 60−86 pmol of the peptide Ile^{244}-Arg^{249} with Trp^{245} again not being detected and corresponded to the peptide of fraction 34 of Figure 4. A following minor peak (fraction 36), not seen in Figure 4, contained about 30 pmol of the overlapping peptide Tyr^{242}-Arg^{249}. Again, Trp^{245} was not detected. Fraction 39 was the apex of the third peak and contained about 25 pmol of the peptide Leu^{121}-Arg^{133} and showed a major decrease in recovery (22 to 1.2 pmol) at Trp^{125} and an impeded tryptic cleavage at Lys^{127}. This peak corresponds to fraction 39 of Figure 4.

To confirm the identity of the NADP$^+$ binding site domain, 0.5 mg of IDH was also photolabeled with [2′-^{32}P]2N$_3$-NADP$^+$, precipitated with PCA, and digested with chymotrypsin to obtain overlapping peptides. The chymotryptic digested protein was subjected to immobilized Al^{3+} affinity chromatography. The flow-through (fractions 3−5) and the

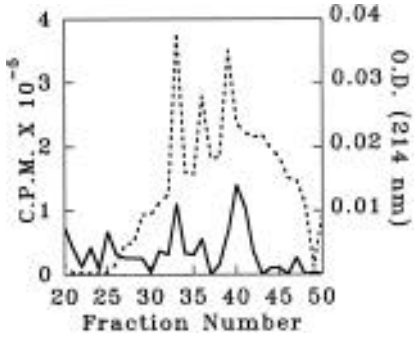

FIGURE 5: HPLC separation of chymotryptic peptides produced from [2′-^{32}P]2N$_3$NADP$^+$ photolabeled IDH after isolation from an immobilized Al^{3+} affinity column as shown in Figure 3. IDH (0.5 mg) in 0.75 mL was photolabeled twice with 30 μM [2′-^{32}P]2N$_3$-NADP$^+$ and proteolyzed by chymotrypsin, and the photolabeled peptides were isolated from bulk peptides by immobilized Al^{3+} affinity chromatography. Phosphate buffer eluted peptides were separated by HPLC as given in Figure 4. The dashed line represents ^{32}P levels obtained per fraction, and the solid line is the OD$_{214}$ absorbance profile.

P$_i$ elution fractions (fractions 16−19) were pooled and concentrated in preparation for reversed phase HPLC. When the flow-through fractions were subjected to reversed phase HPLC, a complex profile was obtained similar to that obtained when the entire chymotryptic digest was chromatographed (data not shown). This, as explained previously, represents the nonphotolabeled peptides that do not bind to the immobilized Al^{3+} affinity column (Shoemaker & Haley, 1996).

Figure 5 shows the radioactivity and absorbance (214 nm) profiles obtained for the P$_i$ eluted fractions when subjected to reversed phase HPLC. The broadness of these peaks is due to the low flow rate which is used to enhance recovery of photolabeled peptide (Haley, 1991). Three major and one minor radioactive peaks were obtained. Again, the first peak eluted at fraction 10 before the acetonitrile gradient was started did not contain any peptides, and is due to the unbound photoprobe not removed in the PCA precipitation step. The fractions at the apex with the maximum radioactivity of other three peaks, peak 2 (fraction 34), peak 3 (fraction 36), and peak 4 (fraction 40), were collected and concentrated under reduced pressure for sequence analysis.

The picomoles of amino acids obtained in each of the peaks are summarized in Table 3. A peptide sequence could

Table 3: Sequence Analysis of the Photolabeled Chymotryptic Peptides of IDH Photolabeled with [2′-^{32}P]2N_3NADP$^+$

cycle	fr[a] 34		fr 40	
1	K^{243} [b]	(30)[c]	L^{121}	(33)
2	I	(12)	V	(0.26)
3	W^{245}	(10)	P	(28)
4	Y^{246}	(9)	G	(13)
5	E	(9)	W^{125}	(2)
6	H^{248}	(1)	T	(15)
7			K^{127}	(10)
8			P	(7)
9			I	nd
10			T	nd
11			I	(7)
12			G	(8)
13			R^{133}	nd
14			H^{134}	(0.4)

[a] fr, fraction no. [b] Superscript identifies primary sequence location. [c] Numbers in parentheses are picomoles of residue obtained.

not be obtained from the minor peak (fraction 36) due to low peptide levels. Fraction 34 contained about 30 pmol of the peptide Lys^{243}-His^{248}. This peptide overlapped with the peptide Tyr^{242}-Arg^{249}, obtained with trypsin digestion. Also, Trp^{245} and Tyr^{246} were not cleaved by chymotrypsin. Fraction 40 contained the peptide Leu^{121}-Ala^{135} which overlaps the tryptic peptide Leu^{121}-Arg^{133}. Again, Trp^{125} showed reduced levels and was not cleaved by chymotrypsin. Trp^{125} is just one amino acid residue away from Lys^{127} which was not cleaved by trypsin. Amino acid residues at positions 9, 10, and 13 were not detected in the analysis due to technical problems with the sequencer.

To demonstrate that NADP$^+$ could reduce the photolabeling of the binding site peptide, IDH (100 μg) was photolabeled with 70 μM [2′-^{32}P]2N_3NADP$^+$ in a total volume of 100 μL, either in the absence or in the presence of 1.5 mM NADP$^+$. The photolabeled IDH was precipitated with PCA and digested with trypsin overnight. The digested protein was diluted with solvent A (0.1% trifluoroacetic acid) and was subjected to reversed phase HPLC. The same three peptide containing peaks, peak 2 (fraction 34), peak 3 (fraction 36), and peak 4 (fraction 40) seen in Figure 5, were obtained, and all were reduced to base-line levels by the addition of NADP$^+$ as observed in Figure 4 using NAD$^+$ (data not shown).

Both 8N_3ATP and 2N_3ATP mimicked ATP in reducing [2′-^{32}P]2N_3NADP$^+$ photoinsertion into IDH. Also, photolabeling of IDH by 10 μM [^{32}P]8N_3ATP was reduced 95%, 88%, and 86% by NADP$^+$, ADP, and ATP, respectively. Photoinsertion by [^{32}P]2N_3ATP was also reduced more effectively by NAD$^+$ and NADP$^+$ than by ATP. To determine if this reduction was caused by ATP binding at an allosteric site or by direct competition at the NADP$^+$ site, [^{32}P]8N_3ATP and [^{32}P]2N_3ATP were used to isolate the peptides with the ATP interacting site. IDH (1 mg) was photolabeled two times using 50 μM probe (about half saturation value) in the presence and absence of 1.6 mM ATP. Trypsin generated peptides were isolated using immobilized Al^{3+} chromatography and HPLC as described above. The HPLC radioactive level and absorbance profile are shown in Figure 6 for the [^{32}P]8N_3ATP experiment and indicate about an 84% reduction in photolabeled peptide in fraction 31 by the addition of ATP. [^{32}P]8N_3ATP photoinserted into a single peptide corresponding to Lys^{243}-His^{248}

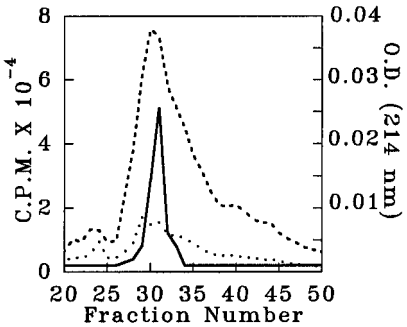

FIGURE 6: HPLC separation of tryptic peptides produced from [α-^{32}P]8N_3ATP photolabeled IDH after isolation from an immobilized Al^{3+} affinity column. IDH (1 mg) was photolabeled twice with 50 μM [^{32}P]8N_3ATP in the presence or absence of 1.6 mM ATP and proteolyzed by trypsin, and the photolablеld peptides were isolated from bulk peptides by immobilized Al^{3+} affinity chromatography. Phosphate buffer eluted peptides were separated by HPLC as given in Figure 4. The bottom dashed and top dashed lines represent ^{32}P levels obtained per fraction with and without ATP present. The solid line is the OD_{214} absorbance profile without ATP present. No OD_{214} peaks were detected with ATP present.

(33 pmol) and again Trp^{245} detection was greatly reduced to 1.3 pmol.

Repeating the above experiment, only using either [α- or [γ-^{32}P]2N_3ATP, two major photolabeled peaks at fractions 33 and 38 were detected. In fraction 33 a single peptide corresponding to Ile^{244}-Arg^{249} (22 pmol) was identified, again with Trp^{245} being nondetectable. In fraction 39 lesser amounts (8 pmol) of an additional overlapping peptide corresponding to Thr^{238}-Arg^{249} were identified. In this latter peptide Trp^{245} was detected at levels corresponding to the other residues, but Tyr^{242} was not detected and tryptic cleavage at Lys^{243} did not occur. Fraction 38 also contained a third peptide (5−8 pmol) identical to the peptide identified using [^{32}P]2N_3NAD$^+$ and [2′-^{32}P]2N_3NADP and corresponding to Leu^{121}-Lys^{127}, with Trp^{125} not being detected (data not shown).

DISCUSSION

Azidopurine photoaffinity analogs have been used effectively to isolate the base binding domains of nucleotide binding site peptides of many enzymes (Kim & Haley, 1991; Shoemaker & Haley, 1993, 1996; Chavan et al., 1992; Olcott et al., 1994). With creatine kinase the peptides identified by photolabeling (Olcott et al., 1994) were later confirmed as being within the adenine binding domain by X-ray crystallography (Fritz-Wolf et al., 1996). [2′-^{32}P]2N_3NADP$^+$ has been synthesized recently and used to monitor the purity of the enzyme 5α-reductase through the different purification steps and isolate the active site peptides (Bhattacharyya et al. 1994, 1995). With every dehydrogenase where the azidopurine analogs have been used they have been found to bind to the NAD(P)$^+$ site with higher affinity than the native nucleotide. This is probably due to the azide conferring a more favorable conformation and is likely the reason that even the 8- and 2-azido-ATP analogs bound much tighter to NADP$^+$-dependent IDH than did ATP. This tighter binding enhances the utility of these analogs as photoaffinity probes. In this report, [2′-^{32}P]2N_3NADP$^+$ was used to isolate overlapping tryptic and chymotryptic peptides of the adenine ring binding domain of the NADP$^+$ binding site of porcine heart mitochondrial NADP$^+$-dependent IDH. Corresponding

data using [^{32}P]2N_3NAD$^+$ confirmed the results obtained using [2′-^{32}P]2N_3NADP$^+$.

Under the experimental conditions described, the photoinsertion into IDH saturated at about 100 μM [2′-^{32}P]2N_3-NADP$^+$. The apparent K_d of this interaction was 14 $\pm$ 3 μM. The specific reduction of photoinsertion of [2′-^{32}P]2N_3-NADP$^+$ (10 μM) by NADP$^+$ demonstrated that the photoprobe is inserting into a specific NADP$^+$ site within IDH. NAD$^+$ could also reduce photolabeling with this probe, but was not as effective as NADP$^+$. Correspondingly, [^{32}P]2N_3-NAD$^+$ photoinserted into IDH, showing saturation effects with reduction of photoinsertion effected best by NADP$^+$ versus NAD$^+$. ATP could also reduce the photolabeling with this probe, but was not as effective as either NAD$^+$ or NADP$^+$. Earlier experiments have shown that NAD$^+$ is a weakly interacting substrate and that both NAD$^+$ and ATP are inhibitors for NADP$^+$-dependent IDH (Kornberg & Pricer, 1950; Ehrlich & Colman, 1978). However, the initial experiments were done at relatively high ionic strengths, and later research has shown that the dissociation constant for NADPH decreased about 1000-fold in going from 0.336 to 0.036 M ionic strength (Mas & Colman, 1985). In all photolabeling experiments, the ionic strength was kept low to enhance binding affinity, as we have also observed in general that the lower the ionic strength the tighter the binding of nucleotide photoaffinity probes and the more efficient the photoinsertion. Therefore, the reported apparent K_ds obtained from photoaffinity labeling should be interpreted considering that photolabeling is done under conditions that enhance binding site occupancy. Specifically, comparison of K_d values for IDH from different studies should be done with caution since ionic strength, pH, and different ionic species are known to cause considerable differences in affinity (Mas & Colman, 1985).

Interaction within the active site was demonstrated since photolabeling in the presence of 136 μM [^{32}P]2N_3NAD$^+$ resulted in approximately a 50% loss of IDH activity as measured by the formation of NADPH as well as demonstrating about 50% photoinsertion efficiency. Photolysis without photoprobe present caused no loss of activity. Also, the presence of 1 mM NADP$^+$ or NAD$^+$ prevented detectable loss of enzyme activity caused by photolysis with 136 μM 2N_3NAD$^+$ under conditions identical to that used to photolabel and inhibit the enzyme 50%.

The isolation of over 90% of the photolabeled peptides by immobilized Al^{3+} or boronate chromatography (detected as ^{32}P at levels of 10^6 or higher) led to the isolation of only two peptide domains. Overlapping tryptic and chymotryptic peptides confirmed and narrowed the peptide regions being photomodified. No other peptides were detected in these fractions. Also, calculation of the amount of photolabeled peptide using the specific activity of the photoprobe and the amount of radiolabel in the sequencing fraction proved that the preponderance of peptide in the fraction was photolabeled. This confirms that prior treatment with the immobilized Al^{3+} or boronate columns retained and led to the isolation of primarily photolabeled peptides. This greatly reduces the possibility of any non-photolabeled peptide coeluting on HPLC with the photolabeled peptide, which could give misleading results.

The photoinsertion site of [2′-^{32}P]2N_3NADP$^+$ and [^{32}P]2N_3-NAD$^+$ into IDH has been identified as the domains containing residues Ile^{244}-Arg^{249} and Leu^{121}-Lys^{127}. This was verified using two different proteases to obtain overlapping peptides. These peptide sequences are conserved between the porcine heart mitochondria, bovine kidney mitochondria, and yeast NADP$^+$-dependent IDH enzymes, but not between related IDHs of *E. coli* and *Thermus thermphilus* (Haselback et al., 1992; Huh et al., 1993). The location of the sites of photoinsertion and the tryptic peptides is shown within the entire sequence in Figure 7.

ADQRIKVAKP VVEMDGDEMT RIIWQFIKEK LILPHVDVQL 40

KYFDLGLPNR DQTNDQVTID SALATQKYSV AVKCATITPD 80

EARVEEFKLK KMWKSPNGTI RNILGGTVFR EPIICKNIPR 120

LVPG*W*TK*P*IT IGRHAHGDQY KATDFVVDRA GTFKIVFTPK 160

DGSSAKQWEV YNFPAGGVGM GMYMTDESIS GFAHSCFQYA 200

IQKKWPLYMS YKNTILKAYD GRFKDIFQEI FEKHYKTDFD 240

KY*K*I*W*Y*E*HRL IDDMVAQVLK SSGGFVWACK NYDGDVQSDI 280

LAQGFGSLGL MTSVLVCPDG KTIEAEAAHG TVTRHYREHQ 320

KGRPTSTNPI ASIFAWTRGL EHRGKLDGNQ DLIRFAQTLE 360

KVCVETVESG AMTKDLAGCI HGLSNVKLNE HFLNTSDFLD 400

TIKSNLDRAL GRQ 413

FIGURE 7: Sequence of porcine mitochondrial IDH (Haselbeck et al., 1992; Huh et al., 1993). Proposed residues modified by photoinsertion, W^{125} and W^{245}, are underlined; sites of impeded tryptic cleavage, K^{127} and K^{243}, and impeded chymotryptic cleavage, Trp^{246}, are shown in italics. Tryptic peptides isolated and sequenced are shown in bold.

There is sometimes a lability of the bond generated by photoinsertion observed during HPLC. When this occurs, it is difficult to determine the exact amino acid residue(s) photomodified (King et al., 1991; Haley, 1991; Shoemaker & Haley, 1996). The exact amino acid photoinserted into is usually identified when no residue is detected in a specific cycle of the sequencing of the photolabeled peptide, especially when the sequence is known and the expected residue is one easily detected. Fortunately, IDH seems to be a situation where the photoinserted label is relatively stable. This seems to fit the general situation where photoinsertion into aromatic or lysine residues generates an adduct that is relatively stable to HPLC and the residues modified are easily identified. However, even when HPLC unstable insertions are obtained, there is a way to detect the probable site of photomodification since the results of treatment of the photolabeled protein with digestive enzymes can be affected. For example, the photomodification of the protein at a particular amino acid, such as Lys for trypsin or Trp for chymotrypsin, generates a sterically hindered peptide which will not be cleaved by trypsin or chymotrypsin, respectively.

IDH represents a perfect example for this type of cleavage analysis. From Table 2, it can be seen that Trp^{245} was not detected in the first tryptic peptide Ile^{244}-Arg^{249} of [^{32}P]2N_3-NAD$^+$ and [2′-^{32}P]2N_3NADP$^+$ photolabeled IDH. Also, the overlapping minor tryptic peptide, Tyr^{242}-Arg^{249}, is an extended version of peptide Ile^{244}-Arg^{249} where tryptic cleavage at Lys^{243}, just one residue away from Trp^{245}, did not occur. It is likely that photoinsertion into Trp^{245} decreases recovery of Trp^{245} and reduces tryptic cleavage at Lys^{243}. Further, in the second tryptic peptide, Leu^{121}-Arg^{133}, there is a major decrease in Trp^{125} and Lys^{127} was not readily cleaved by trypsin. With [^{32}P]2N_3NAD$^+$ photolabeled IDH,

about 30−50 pmol of peptide cleaved at Lys^{127} versus 600−700 pmol of peptide not cleaved at Lys^{127} were obtained. A comparison of the tryptic fragments from [^{32}P]2N_3NAD$^+$ versus [2′-^{32}P]2N_3NADP$^+$ photolabeled IDH suggests that the 2′-phosphate interacts with Lys^{241}, slowing down the rate of cleavage at this residue (see Table 2).

Further support for the site of photoinsertion is found in Table 3, where it is observed that chymotrypsin cleaved effectively at Tyr^{242} but did not cleave at Trp^{245} or the adjacent $Tyr^{246}$of peptide Lys^{243}-His^{248}. Also, Trp^{125} of the second eluted peptide, identified as Leu^{121}-through Gly^{132} before loss of reliability, showed reduced detection and was not cleaved by chymotrypsin. Trp^{125} is just two residues away from Lys^{127} which was not cleaved by trypsin in the first experiments. This again indicates that the site of photomodification by [2′-^{32}P]2N_3NADP$^+$ is probably near Trp^{245}-Tyr^{246} and Trp^{125}-Lys^{127}.

A similar situation was observed earlier concerning the GTP site of GDH where Lys^{445} was not detected during sequencing and trypsin did not cleave at this particular residue as it should (Shoemaker & Haley, 1993). This has also been observed in the related situation of diphtheria toxin in which NAD$^+$ protects Lys^{39} from trypsin digestion (Zhao & London, 1988). Also, with *Clostridium botulinum* C3 ADP-ribosyltransferase, overlapping tryptic and V8 protease peptides were isolated with Trp^{18} of the sequence $Lys^{16}Lys^{17}$-Trp^{18} not being detected, and these lysines were not cleaved by trypsin, likely due to the photoinsertion into Trp^{18} sterically intefering with the digestion procedure (Chavan et al., 1992). This appears to be a generally applicable approach to determining the site of photomodification into enzymes. Therefore, Trp^{245} and Trp^{125} residues are excellent candidates for the site of photoinsertion with [^{32}P]2N_3NAD$^+$ and [2′-^{32}P]2N_3NADP$^+$ since chymotrypsin did not cleave at these nondetected residues and trypsin did not cleave at the nearby Lys^{243} and Lys^{127} residues.

This result is logical since the presence of a Trp residue appears to be a common feature observed in the NAD$^+$ binding sites of many toxins and it has been suggested that the adenine ring of NAD$^+$/NADP$^+$ stacks with the indole ring of Trp. For example, Trp^{50} in diphtheria toxin and Trp^{18} in C3 ADP-ribosyltransferase have been suggested to be involved in stacking with the adenine ring of NAD$^+$ (Chavan et al., 1992; Zhao & London, 1988). Similarly, it is very likely that the Trp residues, Trp^{245} and Trp^{125}, in IDH may be involved in stacking with the adenine ring of NADP$^+$.

The identification of Trp^{245} and Trp^{125} as interacting residues with the adenine ring of NADP$^+$ appears to be in contrast to another study using the adenine ring modified chemical probe of NADP$^+$, 2-[(4-bromo-2,3-dioxobutyl)-thio]-1,N^6-ethenoadenosine 2′,5′-bisphosphate, where the NADP$^+$ binding region was reported to contain the peptide Asp^{375}-Leu^{387} (Bailey & Colman, 1987). This same peptide was also isolated using a substrate analog [^{14}C]-3-bromo-2-ketoglutarate (Erlich & Colman, 1987). This was explained by suggesting that while the adenosine ribose part of the NADP$^+$ affinity label is physically present at the coenzyme site, it reacts at the substrate site. However, chemically reactive probes, due to their long-lived reactive state, have an increased opportunity to react with the most nucleophilic residues within an enzyme and may not necessarily react with a less reactive or nonreactive residue that may be located within the binding domain. This is especially likely if they display low affinity for the binding site being studied.

[2′-^{32}P]2N_3NADP$^+$ is a probe that, on photolysis, generates a very reactive nitrene that has the capability of photoinserting into any residue. Also, the nitrene half-life is so short-lived that prephotolysis of the probe followed by immediate addition of IDH results in no photoinsertion. The data showing decreased photoinsertion by addition of NAD$^+$ or NADP$^+$ demonstrates that photoinsertion occurs only by the bound form of [2′-^{32}P]2N_3NADP$^+$. This indicates that proximity controls photoinsertion and that the residues modified are within the adenine binding domain.

Both α- and γ-^{32}P-labeled 8N_3ATP and 2N_3ATP were used to photolabeled IDH. No phosphorylation was observed with the γ-probe which could be used as effectively as the α-probe. Both [^{32}P]8N_3ATP and [^{32}P]2N_3ATP photoinserted at lower efficiency (about 12%) than [^{32}P]2N_3NAD$^+$, or [2′-^{32}P]2N_3NADP$^+$ and reduction of their photoinsertion was always effected best by NADP$^+$. Also, the observed reduction in photoinsertion of [^{32}P]2N_3NAD$^+$ and [2′-^{32}P]2N_3NADP$^+$ by ATP, 8N_3ATP, and 2N_3ATP further indicated that the triphosphates compete at the NADP$^+$ binding site but with less affinity than NAD$^+$ or NADP$^+$. This was confirmed by isolating the peptides photolabeled by [α-^{32}P]8N_3ATP and [γ-^{32}P]2N_3ATP. Interestingly, photomodification with [α-^{32}P]8N_3ATP resulted in only one photolabeled peptide, Lys^{243}-Arg^{249}, with Trp^{245} showing reduced levels of detection. However, [γ-^{32}P]2N_3ATP photolabeled IDH gave three peptides. The first two were a major (22 pmol) and minor (6−8 pmol) set of overlapping peptides. The major peptide corresponded to Lys^{243}-Arg^{249}, with Trp^{245} not detectable for the major peptide. The minor peptide was Thr^{238}-Arg^{249}, with Tyr^{242} not detected, no cleavage at Lys^{243}, and Trp^{245} present at expected levels. The third peptide corresponded to Leu^{121}-Lys^{127} with Trp^{125} not detected. Identification of these peptides demonstrates that ATP binds at the NADP$^+$ site of IDH but the adenine ring is not as rigidly held in position, resulting in Tyr^{242} also being modified and accounting for the lower efficiency of photoinsertion.

Although the structure of NADP$^+$-dependent IDH from *E. coli* has been well characterized (Hurley et al., 1989), a three-dimensional structure of mammalian heart IDH is unavailable. *E. coli* NADP$^+$-IDH consists of three domains, a large α + β domain, a small α/β domain, and an α/β clasp like domain. NADP$^+$ is bound by the large α + β domain, a structure which has very little similarity to the structure of the nucleotide binding domain of lactate dehydrogenase (LDH)-like family of proteins. The porcine NADP$^+$-IDH shows only 14% amino acid sequence homology to the *E. coli* NADP$^+$-IDH (Haselback et al., 1992). Thus, it is impossible to deduce a reliable structure for the porcine enzyme based on the known structure of the *E. coli* enzyme. Also, since the structure of the mammalian IDH is not known, it is not yet possible to define the NADP$^+$ binding site peptides isolated in this study with respect to the three-dimensional structure. However, many residues in two regions identified by [2′-^{32}P]2N_3NADP$^+$ photolabeling, described as Arg^{120} through Asp^{144} and Glu^{232} through Ala^{256}, are highly conserved in eukaryotic NADP$^+$-dependent IDHs. Specifically, Arg^{120}, Trp^{125}, Lys^{127}, Arg^{133}, His^{248}, and Arg^{249} are totally conserved, whereas Lys^{243} and Trp^{245} were found in two of three IDHs (Huh et al., 1993).

Important mechanism/structural information can be obtained from the analysis of IDH with nucleotide photoaffinity probes. First, the data demonstrate that the $NADP^+$ site of IDH interacts with ATP more readily than does the NAD^+ binding site of GDH, LDH, and the ADP-ribosylating Enzyme 3 of botulinium toxin (Kim & Haley, 1990; Chavan et al., 1992). With porcine IDH, ATP and ATP photoprobes seem to interact, although with less affinity, within the $NADP^+$ binding site as determined by reduction of photoinsertion of $[^{32}P]2N_3NAD^+$ and the isolation of identical peptide regions using $[2'\text{-}^{32}P]2N_3NADP^+$, $[^{32}P]2N_3NAD^+$, $[^{32}P]8N_3ATP$, and $[^{32}P]2N_3ATP$. However, the additional photoinsertion of $[^{32}P]2N_3ATP$ into Tyr^{242} indicates a different geometry of binding of ATP versus $NADP^+$ at this site. This is probably reflective of the lower affinity for ATP and the ATP probes. Therefore, if ATP plays a role in regulation of mammalian IDH activity, it is probably as a competitive inhibitor of $NADP^+$ binding.

Finally, the adenine ring binding domains for both $NADP^+$ and NAD^+ of pig heart IDH appear to consist of two regions of the primary sequence corresponding to peptide Ile^{244}-Arg^{249}, with Trp^{245} being the major site of photoinsertion, and peptide Leu^{121}-Lys^{127}, with Trp^{125} being the site of photoinsertion (see Figure 7). What is not known is if Trp^{245} and Trp^{125} are close in the three-dimensional structure and represent one binding site or represent two distinct sites. A previous report using fluorescence titration techniques has shown a stoichiometry of 0.5 nucleotide binding per subunit whereas UV spectral titration and ultrafiltration gave one nucleotide per subunit, a result that was suggested to be due to different conformational states of IDH (Mas & Colman, 1985). Such different conformational states could also help explain our results. For example, the saturation and protection experiments represented by Figures 1 and 2, respectively, do not show the biphasic characteristic that would be observed if photoinsertion occurred within these concentration ranges at two sites with markedly different affinities (Shoemaker & Haley, 1996). Also, the reduction of about 50% activity with about 50% of the IDH subunits being photolabeled with two photolyses using 130 μM $[^{32}P]2N_3$-NAD^+ agrees with a one site per subunit model with half of the sites being conformationally different and not as susceptible to efficient photolabeling, yet retaining catalytic activity. Photolabeling at just below saturation resulted in about a 1.2:1.0 peptide ratio of Ile^{244}-Arg^{249} to Leu^{121}-Arg^{133} as shown in Table 2, and protection of photoinsertion into both peptides was reduced almost equally by competing $NADP^+$ and NAD^+. These two observations do not conclusively prove the relative geometry of the tryptophans but are consistent with Trp^{245} and Trp^{125} being located within a single three-dimensional binding site.

REFERENCES

Bailey, J. M., & Colman, R. F. (1987) *J. Biol. Chem. 262*, 12620−12626.

Bhattacharyya, A. K., Chavan, A. J., Shuffett, M., Haley, B. E., Collins, D. C. (1994) *Steroids 59*, 634−641.

Bhattacharyya, A. K., Chavan, A. J., Haley, B. E., Taylor, M. F., & Collins, D. C. (1995) *Biochemistry 34*, 3663−3669.

Chavan, A., Nemoto, Y., Narumiya, S., Kozak, S., & Haley, B. E. (1992) *J. Biol. Chem. 267*, 14866−14870.

Colman, R. F. (1972) *J. Biol. Chem. 247*, 215−223.

Colman, R. F. (1983) *Pept. Protein Rev. 1*, 41−69.

Colman, R. F. (1989) *Biochem. Soc. Trans. 17*, 307−311.

Erlich, R. S., & Colman, R. F. (1978) *Eur. J. Biochem. 89*, 575−587.

Erlich, R. S., & Colman, R. F. (1987) *J. Biol. Chem. 262*, 12614−12619.

Fritz-Wolf, K., Schnyder, T., Wallimann, T., & Kabsch, W. (1996) *Nature 381*, 341−345.

Haley, B. (1975) *Biochemistry 14*, 3852−3857.

Haley, B. (1991) *Methods Enzymol. 200*, 477−487.

Haselback, R. J., Colman, R. F., & McAlister-Henn, L. (1992) *Biochemistry 31*, 6219−6223.

Huh, J., Ryu, J.. Huh, J., Sung, H., Oh, I., Song, B. J.,, & Veech, R. L. (1993) *Biochem. J. 292*, 705−710.

Hurley, J. H., Thorsness, P. E., Ramalingam, V., Helmers, N. H., Koshland, D. E., Jr., & Stroud, R. E. (1989) *Proc. Natl. Acad. Sci. U.S.A. 86*, 8635−8639.

Hurley, J. H., Dean, A. M., Koshland, D. E., Jr., & Stroud, R. M. (1991) *Biochemistry 30*, 8671−8678.

Jayaram, B., & Haley, B. E. (1994) *J. Biol. Chem. 269*, 1−10.

Kelly, J. H., & Plaut, G. W. E. (1981) *J. Biol. Chem. 256*, 335−342.

Kim, H., & Haley, B. (1990) *J. Biol. Chem. 265*, 3636−3641.

Kim, H., & Haley, B. (1991) *Bioconjugate Chem. 2*, 142−147.

King, S., Kim, H., & Haley, B. E. (1991) *Methods Enzymol. 196*, 449−466.

Kornberg, A., & Pricer, W. E., Jr. (1951) *J. Biol. Chem. 189*, 123−136.

Laemmli, U. K. (1970) *Nature 227*, 680−685.

LaPorte, D. C., & Koshland, D. E., Jr. (1983) *Nature 305*, 286−290.

Mas, M. T., & Colman, R. F. (1985) *Biochemistry 24*, 1634−1646.

Northrop, D. B., & Cleland, W. W. (1974) *J. Biol. Chem. 249*, 2928−2931.

Olcott, M., Bradley, M., & Haley, B. (1994) *Biochemistry 33*, 11935−11941.

Potter, R., & Haley, B. (1982) *Methods Enzymol. 91*, 613−633.

Salvucci, M., Chavan, A., & Haley, B. (1992) *Biochemistry 31*, 4479−4487.

Shoemaker, M. T., & Haley, B. E. (1993) *Biochemistry 32*, 1883−1890.

Shoemaker, M., & Haley, B. (1996) *Bioconjugate Chem. 7*, 302−310.

Soundhar, S., & Colman, R. F. (1993) *J. Biol. Chem. 268*, 5264−5271.

Stoddard, B. L., & Koshland, D. E., Jr. (1993a) *Biochemistry 32*, 9310−9316.

Stoddard, B. L., & Koshland, D. E., Jr. (1993b) *Biochemistry 32*, 9317−9322.

Trad, C., Chavan, A., Clemens, J., & Haley, B. (1993) *Arch. Biochem. Biophys. 304*, 58−64.

Uhr, M. L., Thompson, V. W., & Cleland, W. W. (1974) *J. Biol. Chem. 249*, 2920−2927.

Zhao, J., & London, E. (1988) *Biochemistry 27*, 3398−3403.

BI9614592